679

UCRL-51523

HIGH-PRESSURE MECHANICAL PROPERTIES OF KAYENTA SANDSTONE

A. G. Duba, A. E. Abey, B. P. Bonner, H. C. Heard,
and R. N. Schock

February 5, 1974

Prepared for U.S. Atomic Energy Commission under contract No. W-7405-Eng-48

LAWRENCE LIVERMORE LABORATORY
University of California/Livermore

Printed in the United States of America
Available from
National Technical Information Service
U. S. Department of Commerce
5285 Port Royal Road
Springfield, Virginia 22151
Price: Printed Copy $___*; Microfiche $0.95

*Pages	NTIS Selling Price
1-50	$4.00
51-150	$5.45
151-325	$7.60
326-500	$10.60
501-1000	$13.60

TID-4500, UC-11
Environmental and
Earth Sciences

LAWRENCE LIVERMORE LABORATORY
University of California Livermore, California 94550

UCRL-51526

HIGH-PRESSURE MECHANICAL PROPERTIES OF KAYENTA SANDSTONE

A. G. Duba, A. E. Abey, B. P. Bonner, H. C. Heard,
and R. N. Schock

MS. date: February 5, 1974

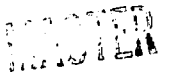

Contents

HIGH-PRESSURE MECHANICAL PROPERTIES OF KAYENTA SANDSTONE

Abstract

Pressure-volume, uniaxial strain loading, uniaxial stress loading to failure, and ultrasonic velocity determinations have been performed on samples of Kayenta sandstone from the site of the Mixed Company event. Hydrostatic pressure of 2 GPa produces about 23% volume compression, with 9% permanent compaction remaining upon unloading. The pressure-volume data indicate that crush-up of porosity begins between 200 and 300 MPa. In uniaxial strain loading, the sandstone loads directly to the vicinity of the failure envelope, then parallels that envelope to the highest confining pressure (480 MPa). At strain rates of about 10^{-4}/s, the loading path in uniaxial strain up to 200 MPa is coincident in pressure-volume space with the shock-loading path (at a strain rate of about 10^{5}/s) observed on samples from the same block. The permanent compaction, after unloading under conditions of uniaxial strain from 625 MPa mean pressure, is about 3.6%. Uniaxial stress loading indicates a brittle-ductile transition between 400 and 500 MPa mean pressure. Between 100 and 500 MPa mean pressure, the slope of the failure envelope is decreased considerably with respect to that below 100 MPa and between 500 and 900 MPa. This plateau, which is not present in the failure envelope for material subjected to a 700-MPa confining pressure before the uniaxial stress test, is interpreted as being due to pore crush-up during hydrostatic loading. As confining pressure is increased from 0.1 MPa to 1 GPa, the measured compressional velocity increases from 3.0 km/s to 5.0 km/s and the shear velocity increases from 1.5 km/s to 2.4 km/s. Small decreases in compressional velocity (~ 5%) between 10 and 40 MPa are attributed to local brittle failure resulting from highly localized stress concentrations within the sample under hydrostatic loading.

Introduction

The mechanical response of materials to the large stress pulses typical of high-energy and nuclear explosives is a matter of importance for site hardening, as well as stemming and containment, in the underground testing program of the Defense Nuclear Agency (DNA). To improve computer modeling techniques and to study the response of a porous sandstone, the Mixed Company event, a well-instrumented experiment using high-energy explosives, was performed at a site in Mesa County, Colorado. As shown in Fig. 1, this site had been

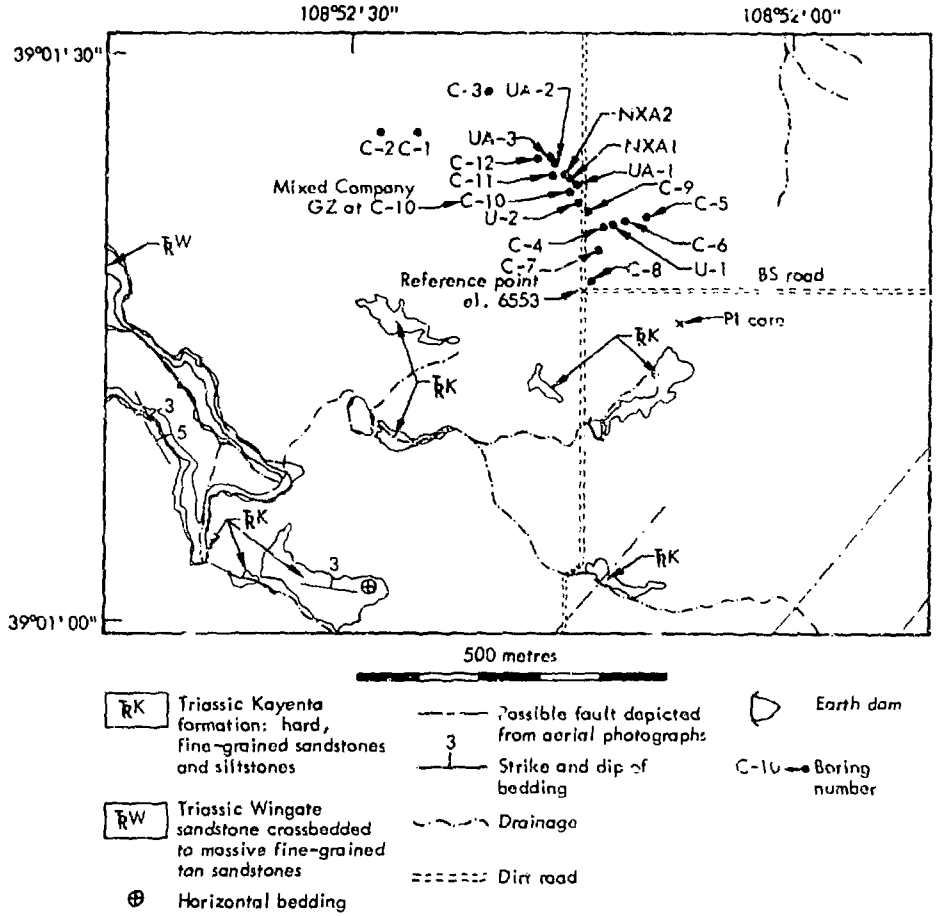

Fig. 1. Map of the Mixed Company site, Mesa County, Colorado, showing the location of the PI core used in this study in relation to ground zero and other sampling in the area. This map is based on preliminary geologic maps of the site area by J. Q. Ehrgott, U.S. Army Engineer Waterways Experiment Station.

extensively sampled to provide material for a variety of equation-of-state (EOS) tests at several strain rates, which were carried out at six laboratories: Stanford Research Institute (SRI), Physics International (PI), Terra Tek Incorporated (TTI), Waterways Experiment Station (WES), Massachusetts Institute of Technology (MIT), and the Lawrence Livermore Laboratory (LLL). This report presents the LLL EOS data on a sandstone from this site.

Data were collected on samples of sandstone prepared from half of a core

(about 355 mm in diameter by 250 mm long), supplied by R. P. Swift of PI. The cylinder was part of core 1-1 from a depth of 6.5 m and about 300 m from the working point ("PI core" in Fig. 1).

The sandstone, from the Kayenta formation, is poorly consolidated and medium- to coarse-grained; it contains more than 90% quartz with a small amount of calcite.[1]

Experimental Procedure

Samples were prepared with diamond coring drills, using water as the coolant. Cores were oven-dried at 80°C for at least 24 hr before density measurements and jacketing. The density of the dry sandstone, as determined by weighing and measuring several samples in air, was 2.04 ± 0.03 Mg/m^3. A dry grain density of 2.688 Mg/m^3 was measured using a helium densitometer on samples ground to pass a 44-μm sieve.[1] The porosity is thus about 24%.

Right circular cylinders varying from 20 to 30 mm in diameter and 30 to 100 mm in length were deformed in a variety of tests. The pressure-volume (P-V) relationship was measured to 1.4 GPa under hydrostatic conditions and to 3.0 GPa under quasi-hydrostatic conditions. The intrinsic compressibility of this rock was determined to 4.0 GPa on a sample which had been ground to pass a 44-μm sieve, mixed with equal parts tin, and hot-pressed at 150°C and 2 GPa into the form of a quasi-static P-V sample. The failure envelope in compression was determined to 1.05 GPa mean pressure from uniaxial stress tests; tensile strengths were determined by the Brazil test at 0.1 MPa. Using foil strain gages, the stress-strain response of this sandstone was monitored under conditions of uniaxial stress and uniaxial strain loading. Shear and compressional velocities (resonant frequency, 1 MHz) were measured to 1.0 GPa confining pressure. All tests were performed at strain rates of about 10^{-4}/s. Experimental techniques employed in this study are discussed in greater detail elsewhere.[2-7]

Test Results

PRESSURE-VOLUME MEASUREMENTS

The pressure-volume (P-V) relationship was determined to 1.4 GPa on jacketed, 32-mm-diam by 76-mm-long specimens immersed in a hydrostatic pressure fluid. Axial and circumferential strain gages were bonded to the jackets to monitor volume changes. Because lead jackets on this very porous, coarse-grained sandstone tended to puncture at pressures above 100 MPa, a special dual-jacketing technique was developed, in which 0.5-mm-thick lead jackets were applied over 0.1-mm-thick copper sheaths. Before strain gages

were applied, thi[illegible]ual jacket was fitted to the rock by 0.4 MPa hydrostatic pres[illegible]are to ensure that the displacement of the jacket would accurately reflect strains in the rock during testing.

Figure 2 shows the P-V relationship to 3.0 GPa as determined from five samples loaded hydrostatically to 1.4 GPa and four samples load[illegible]d under quasi-hydrostatic conditions to 3.0 GPa. Between 0.3 and 1.4 GPa, the data from both types of test are in good agreement. Below 0.2 MPa, hydrostatic data were favored in drafting the figure. Except for one sample tested hydrostatically, which had 5% less compression at 1.0 GPa, the results for all measurements fall within the error bars shown in Fig. 2.

By 3.0 GPa the Kayenta sandstone has undergone 23 ± 1.5% volume compression. On release of pressure from 3.0 GPa, this sandstone has 9% permanent compaction. The P-V relationship as determined from another core from the same sampling site[8] is included in Fig. 2. The two determinations are in excellent agreement below 300 MPa, but they diverge above this pressure, where crush-up was observed to occur in the present study.

The P-V curve has a rather complex shape. Beginning with a low [illegible]tial slope, which is probably the result of closing of cracks with low aspect ratio, the bulk modulus (K) increases until pore crush-up begins (between 200 and

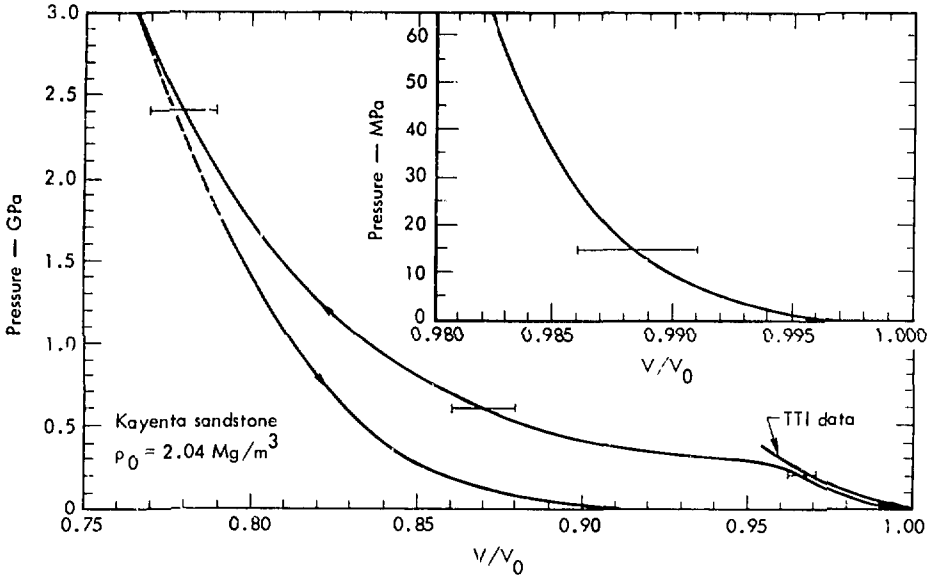

Fig. 2. Pressure-volume relationship for dry Kayenta sandstone. The insert shows behavior in the first 60 MPa. Data from TTI (Ref. 8) on sandstone from the Mixed Company site are included for comparison.

300 MPa). Over the pressure interval of 300-400 MPa, an additional 5% volume compression occurs, yielding a low bulk modulus. From 0.4 to 3.0 GPa, the slope of the P-V curve increases smoothly. Table 1 lists bulk moduli calculated from the slopes of the P-V curve in Fig. 2. The complex variation of bulk modulus with pressure to 800 MPa is displayed graphically in Fig. 3.

Figure 4 compares the specific volume ($\bar{\nu}$) of the Kayenta sandstone with the intrinsic compressibility determined on a powdered sample. Although the specific volumes differ by almost 3% at 3 GPa, the slopes are similar. The slope for the sandstone is slightly less

Table 1. Bulk modulus of Kayenta sandstone.

Pressure (MPa)	Bulk modulus, K (GPa)
0.1	0.6
2	1.2
5	2.5
10	4.2
30	6.8
150	9.8
270	4.0
350	1.0
500	8.5
1000	14.1
2000	33.7
3000	46.7

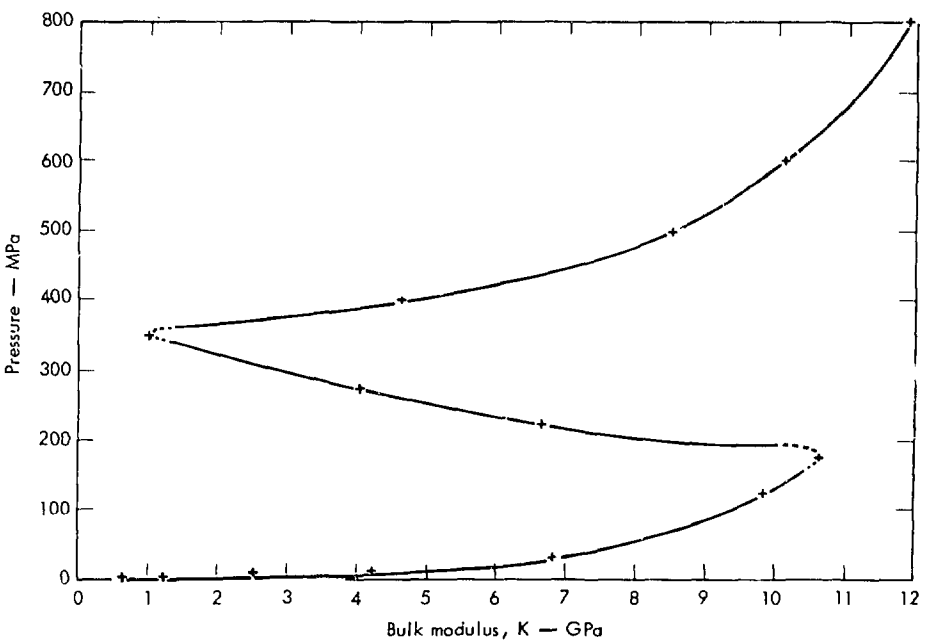

Fig. 3. Bulk modulus as a function of pressure.

than the slope for the powder. This implies that there is 6 to 8% porosity remaining in the rock and that some porosity will persist to pressures of 10 GPa. Below 2 GPa, pore crush-up and crack closure dominate the P-$\bar{\nu}$ relationship in the rock.

Since the Kayenta sandstone is composed mainly of quartz, the intrinsic compressibility is also compared with that of quartz[9] in Fig. 4. The higher initial specific volume of the Kayenta sandstone is due to the presence of calcite and other impurities including a possible small amount of magnetite.[1] These impurities are also consistent with the slightly higher compressibility of the intrinsic P-$\bar{\nu}$ curve compared with that of quartz.

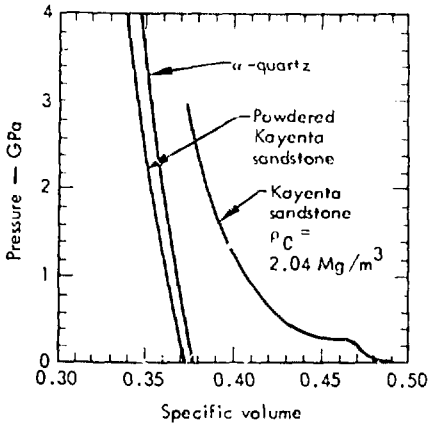

Fig. 4. Specific volume of Kayenta sandstone compared with the specific volume of powdered Kayenta sandstone and quartz.

UNIAXIAL STRESS MEASUREMENTS (FAILURE)

Both uniaxial compression and indirect tension (Brazil) tests were made on the dry Kayenta sandstone. In the former, Tygon-jacketed cylindrical samples (19 mm in diameter by 40 mm long) were compressed to failure at confining pressures ranging to 700 MPa. Tensile strengths were determined at atmospheric pressure in the Brazil test by compressing a cylindrical sample along its diameter.

Data were taken in the form of force-displacement curves. After calculation to differential-stress vs axial-strain curves, either the ultimate strength (in those tests which showed brittle behavior) or the differential stress taken at 5% strain (for those samples which were macroscopically ductile) was recorded. The values of the principal stresses at failure for each test (as defined above) are summarized in Table 2.

Brittle failure is characterized by a sudden decrease in the slope of the stress-strain curve at the yield point, followed either by a complete loss of cohesion of the material with a subsequent drop in differential stress to zero, or by continual fracturing and rehealing of the material, characterized by sharp downward breaks in the stress-strain curve. Ductile failure is defined as the absence of any sharp downward breaks in the stress-strain curve beyond the yield point, with the material undergoing at least 5% permanent strain before fracture. On the scale of the test sample, ductile behavior may result from homogeneously distributed microfractures with consequent small rotations of grains or by plastic flow (twinning or translation) on any scale.

Table 2. Summary of uniaxial stress tests of dry Kayenta sandstone.

Principal stresses (MPa)			Shear strength, τ (MPa)	Mean pressure, P_m (MPa)	Behavior
σ_1	σ_2	σ_3			
Brazil tests					
4.2	0.1	-1.4	2.8	9	Brittle
4.8	0.1	-1.6	3.2	11	Brittle
Uniaxial stress tests					
32	0.1	0.1	16	11	Brittle
32	0.1	0.1	16	11	Brittle
148	25	25	62	66	Brittle
223	50	50	87	108	Brittle
310	100	100	105	170	Brittle
453	200	200	126	284	Transitional
600	300	300	150	400	Ductile
794	400	400	197	531	Ductile
1040	450	450	295	647	Ductile
1330	500	500	415	777	Ductile
1334	500	500	417	776	Ductile
1511	600	600	455	904	Ductile
1459	600	600	430	886	Ductile
1735	700	700	517	1045	Ductile
Uniaxial stress tests on samples prepressurized to 700 MPa					
346	100	100	123	182	Ductile
587	200	200	194	329	Ductile
908	300	300	304	503	Ductile
806	300	300	253	469	Ductile
1029	400	400	315	610	Ductile
1148	450	450	349	683	Ductile

In Fig. 5, the shear strength, τ, is plotted against mean pressure, P_m, as calculated from the principal stresses listed in Table 2. Results from each test are shown as open circles; the solid curve is the locus of these data. The transition from brittle fracture to macroscopic ductile flow in this sandstone occurs at 450-500 MPa. At mean pressures between 150 and 750 MPa there is a distinct dip in the failure envelope, with a near-plateau between 200 and 500 MPa. This feature has been observed in the same pressure range in poorly consolidated, high-porosity tuffs.[10,11] In those studies this behavior was attributed to progressive collapse of the matrix framework into the existing pore volume. At higher mean pressures, the tuffs increase rapidly in strength.

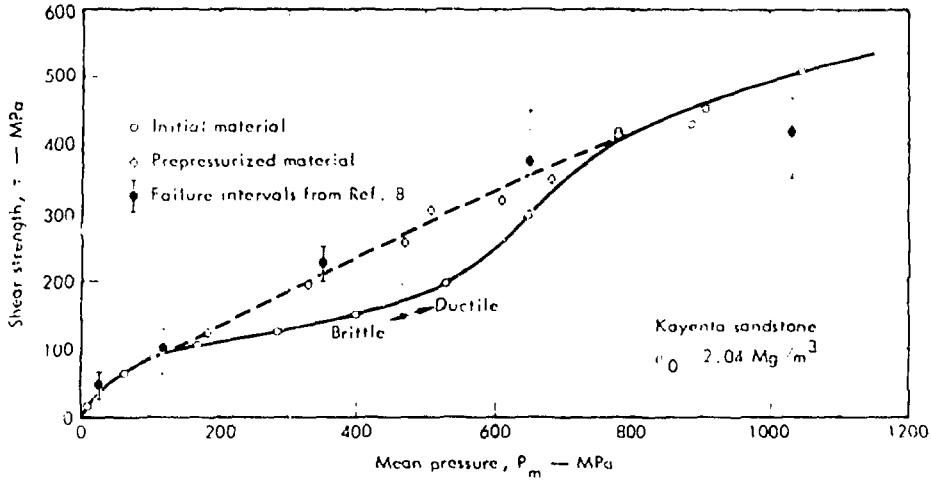

Fig. 5. Shear-strength-vs-mean-pressure failure envelope for dry Kayenta sandstone. The prepressurized samples were pressurized to $\sigma_1 = \sigma_2 = \sigma_3 = 700$ MPa. Failure intervals determined by TTI (Ref. 8) on sandstones from the Mixed Company site are included.

presumably because of the increased bulk density and the more interlocking packing of component grains as a result of the decrease in the pore volume fraction.[10]

This hypothesis relating the plateau in the failure envelope to pore collapse was tested on the Kayenta sandstone. Before the standard testing sequence,[4] each sample was pressurized to 700 MPa confining pressure (Fig. 2 shows that significant porosity is removed by this pressure) and held at that pressure for 10 min. Then confining pressure was lowered to the desired value and the sample was tested according to the standard procedure.

The results for individual specimens are reported in Fig. 5, and the resulting failure envelope is shown by the dashed line. All of the precompressed samples underwent ductile failure. Thus, the brittle-ductile transition occurs at a much lower mean pressure (≤130 MPa) for the prepressurized Kayenta sandstone than for that which had no previous higher-pressure history (470 MPa). It is readily apparent that the hydrostatic pretreatment completely erases any trace of a plateau in the failure surface and the surface becomes monotonic with a slope decreasing with mean pressure. This is the usual behavior for most rocks,[4,6,12,13] in which porosity effects are not dominant over a narrow pressure interval. We thus conclude that the plateau in the failure envelope between 150 and 550 MPa is caused by a catastrophic matrix collapse into existing pore space.

The shear strength of this sandstone below 600 MPa mean pressure, among the lowest we have observed for any dry sandstone,[14] is likely the consequence of the anomalous matrix-pore interaction

discussed above. At pressures above the plateau region, the Kayenta sandstone rapidly attains a more normal strength behavior.

Also plotted in Fig. 5 are failure data of Green et al.[11] for several other core samples taken from the Mixed Company site. The bars indicate the range of failure strength found for samples with density varying from 1.95 to 2.30 Mg/m^3. Included among these are measurements on material from the same core used in this study. Below 1000 MPa mean pressure, except for the plateau region where apparent crush-up lowers the failure envelope in the present study, the data agree within experimental scatter. At higher pressures, the results of Green et al.[11] may somewhat underestimate the strength of the Kayenta sandstone.

THREE DIMENSIONAL STRESS-STRAIN MEASUREMENTS

Foil strain gages, bonded to jacketed cylinders (19 mm in diameter by 40 mm long) of the Kayenta sandstone, monitored the induced strains in this rock under conditions of both uniaxial stress loading to failure and uniaxial strain loading and unloading. In uniaxial stress loading, axial load is increased while constant confining pressure is maintained. In uniaxial strain loading, constant circumferential strain is maintained by increasing the confining pressure as the axial stress is increased. This latter loading path is assumed to model loading during the passage of a plane shock wave. However, the strain rates during shock loading are about 10^6-10^{10} times greater than those employed in these laboratory tests. In both uniaxial strain and uniaxial stress loading, the principal strains are measured to determine loading moduli as functions of deviatoric stress and confining pressure along different loading paths. Samples for the uniaxial stress tests were jacketed with 0.5-mm-thick lead jackets seasoned to 0.4 MPa before installation of strain gages. These jackets maintained their integrity adequately at confining pressures up to 100 MPa.

For the uniaxial strain test, however, jackets made of 0.5-mm-thick lead were not suitable for two reasons: (1) the jacket deformed into the relatively large surface holes of the samples as confining pressure was increased, distorting the strain gages and giving false strain readings, and (2) at pressures greater than about 100 MPa, the jacket was intruded into the surface pores sufficiently to be punctured, thus allowing fluid to enter the rock. Both problems were solved by the use of a 0.1-mm-thick copper sheath beneath the lead jacket. Except for one instance noted in Table 3, jackets were fitted to the rock with 0.4 MPa hydrostatic pressure prior to installation of strain gages. This copper sheath permitted confining pressures of at least 500 MPa to be used without jacket rupture and apparently eliminated spurious strain readings. Below 100 MPa, the data for uniaxial stress loading of single- and double-jacketed specimens agree well (see, for example, Fig. 8 and Table 3). In both uniaxial stress and uniaxial strain loading, the strength of the jackets was taken into account in the data analysis.

Table 3. Moduli and velocities calculated from initial quasi-static loading, Kayenta sandstone.

Jacket material, seasoning pressure	Fig. 8 curve No.	σ_3 (MPa)	Poisson's ratio, ν	Shear modulus, μ (GPa)	Bulk modulus, K (GPa)	Shear velocity, V_s (km/s)	Compressional velocity, V_p (km/s)
Uniaxial strain tests							
Pb, 0.4 MPa	1	0.1	0.23	3.1	4.7	1.23	1.98
Pb, 0.4 MPa	2	0.7	0.14	2.0	2.1	0.99	1.65
Pb + Cu, 0.4 MPa	3	0.5	0.23	3.3	4.9	1.27	2.10
Pb + Cu, 300 MPa	4	0.4	0.20	5.4	7.1	1.62	2.83
Uniaxial stress tests							
Pb, 0.4 MPa		0.1	0.21	2.4	6.0	1.08	2.12
Pb, 0.4 MPa		0.5	0.21	2.5	3.5	1.11	1.83
Pb, 0.4 MPa		20.0	0.30	8.3	17.6	2.02	3.75
Pb, 0.4 MPa		20.0	0.33	7.8	20.0	1.96	3.86
Pb, 0.4 MPa		50.0	0.09	6.5	5.8	1.78	2.66
Pb, 0.4 MPa		100.0	0.17	10.3	12.0	2.24	3.47

Uniaxial Stress

Figure 6 shows stress-strain paths for uniaxial stress tests performed at 0.1, 20, 50, and 100 MPa confining pressure. Duplicate tests were performed at 0.1 and 20 MPa. At confining pressures of 20 MPa and less, this sandstone initially loads above the hydrostat in uniaxial compression. This unusual loading behavior has been observed previously in saturated tuffs[11,15] and was attributed to dilatation on initial loading in these relatively weak tuffs. This behavior is in direct contrast to that observed for less porous sandstones (~10% porosity),[6,14] where shear-enhanced compaction often causes the sandstone to compact below the hydrostat on initial uniaxial stress loading.

The apparent dilatation on initial loading observed at pressures of 20 MPa and less in Fig. 6 is similar to that observed in the saturated tuff from NTS tunnel U12e.06.[15] Both rocks are highly porous and relatively weak in shear. The most plausible explanation for dilatational behavior on initial loading is that, locally, the matrix cement is easily broken with a minimum load and that uncemented grains are able to rotate or translate at low values of applied differential stress. At mean pressures sufficient to induce crush-up, failure of the rock is caused by collapse of grains and matrix into the pore volume, producing only slight dilatation or compaction prior to failure.

At a confining pressure of 100 MPa, only slight initial dilatation is noted; failure occurs after compaction below the hydrostat. At 50 MPa, the rock loads slightly above the hydrostat and

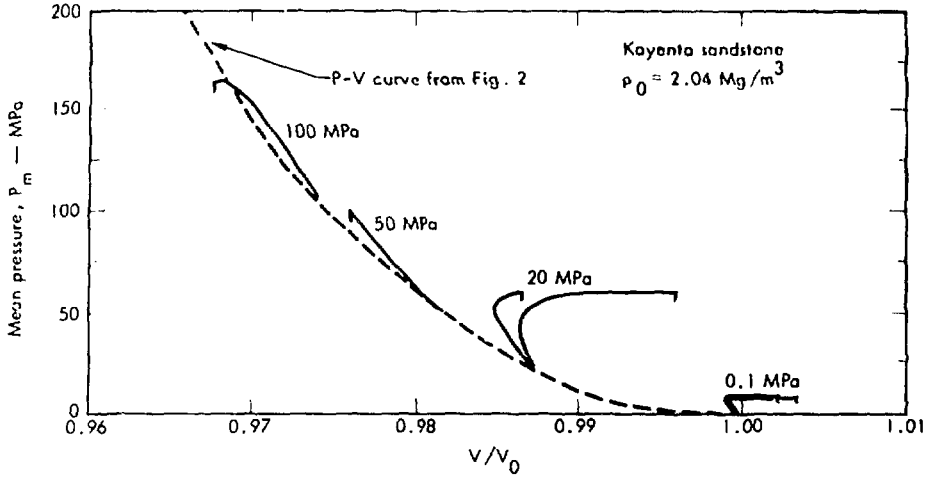

Fig. 6. Volume change as a function of mean pressure in uniaxial stress loading for dry Kayenta sandstone, compared with P-V curve (Fig. 2). Vertical strokes at the ends of the curves indicate fracture of the samples.

tends to diverge from the hydrostat at higher mean pressures. At pressures of 20 MPa and lower, the amount of dilatation prior to failure is noticeably increased. The marked change in behavior between 20 and 100 MPa is probably related to the initiation of the crush-up process in response to the confining pressure. The beginning of the plateau in the failure envelope at 50 MPa confining pressure (Fig. 7 and Table 2) was shown to be related to crush-up of porosity and is consistent with Fig. 6. In addition, the velocity measurements presented below also indicate structural changes in response to confining pressures greater than about 10 MPa. Although the P-V relationship (Fig. 2) shows no gross crush-up prior to about 300 MPa, the uniaxial stress and velocity data indicate that some inelastic behavior is occurring below 50 MPa.

Uniaxial Strain

Figure 7 shows the uniaxial strain path for a sample which was compressed to 5% strain. The sample was rejacketed,

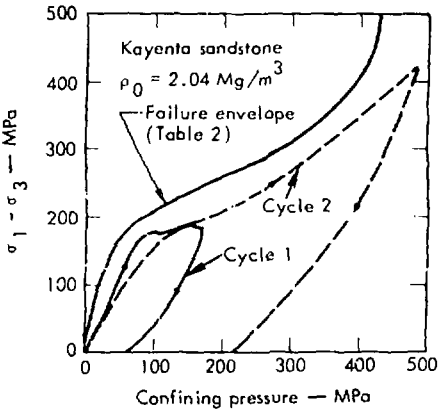

Fig. 7. Stress loading path in uniaxial strain loading for dry Kayenta sandstone, compared to failure envelope (Table 2). Two cycles on the same sample are shown (see text).

regaged and then compressed to an additional 8% strain. As in the tuffs,[10,11,15] the uniaxial-strain loading path of this rock follows slightly below the failure envelope. Based on our experience with the tuffs (wet and dry) and with this sandstone, it appears that rocks which undergo failure by massive pore collapse are typified by uniaxial-strain loading curves that intersect, or nearly intersect, the failure envelope in the plateau region. This is in contrast to the behavior of low-porosity granite (~1% porosity) and graywacke sandstones (~10% porosity), where uniaxial strain loading follows a path whose locus is about half the shear strength.[6,16]

Figure 8 compares P_m vs $-\Delta V/V_0$ for the hydrostat (calculated from Fig. 2) with that for uniaxial strain runs made on four samples. Although the data scatter is relatively large, the uniaxial strain runs show consistent behavior despite variations in jacket material and seasoning pressure noted in Table 3. The loading paths show an initial shallow slope, followed by a steeper region which loads above the hydrostat. This is

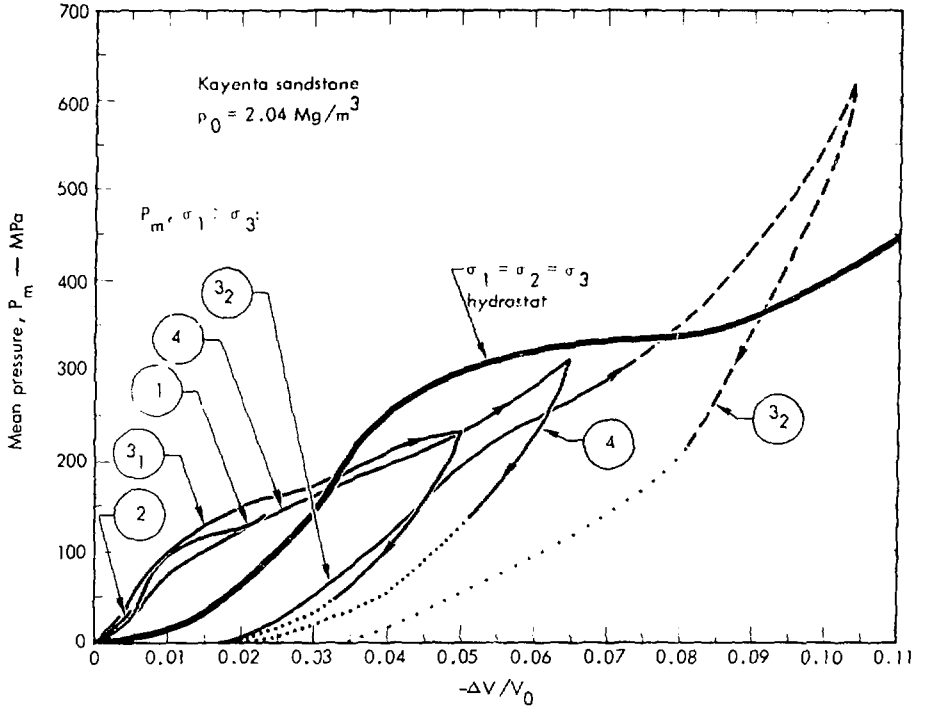

Fig. 8. Volume change as a function of mean pressure in uniaxial strain loading for dry Kayenta sandstone, compared with P-V curve (calculated from Fig. 2). Numerically identified curves refer to Table 3. Dotted portions of the uniaxial-strain unloading paths indicate hydrostatic unloading.

followed by a decrease in slope at about 1% volume strain (P_m varies at this point from 70 to 100 MPa) and an ultimate intersection with the hydrostat at about 3% volume strain (P_m varies from 170 to 190 MPa).

As in the uniaxial stress runs discussed above, shear-enhanced compaction probably does not occur at low mean pressures; rather, the presence of shear stress tends to inhibit compaction in this porous sandstone at mean pressures less than about 150 MPa in uniaxial strain (Fig. 8). At mean pressures greater than about 150 MPa, both uniaxial strain and uniaxial stress tests indicate that this sandstone compacts below the hydrostat. The uniaxial strain data (Fig. 8) indicate significant enhanced compaction up to 300 MPa. The behavior of the sandstone beyond this point is uncertain because the strain gages indicated more than 5% strain, the limit of reliability of our gages. Thus the Kayenta sandstone exhibits shear-enhanced compaction similar to that observed for other, less porous sandstones[6] but at lower pressures. Attempts to gather additional data beyond 5% strain by rejacketing and regaging samples which had been previously subjected to 5% compression in uniaxial strain loading were thwarted by jacket failure. The permanent compaction observed after unloading in uniaxial strain varied from 1.2%, for a sample which had been to 190 MPa mean pressure, to about 2%, for samples which had been to mean pressures of 210 and 310 MPa. For the sample which had been to 600 MPa, the 3.6% permanent compaction is unreliable since the strain gages had been deformed beyond the limit of their reliability.

In Fig. 9, the σ_1 vs $-\Delta V/V_0$ loading path in uniaxial strain as observed at strain rates of $\sim 10^{-4}$/s is compared with the two loading paths observed at strain rates of $\sim 10^{5}$/s on material from the same block.[17] The agreement up to 250 MPa is surprisingly good. Apparently, the response of this sandstone to σ_1 loading is strain-rate independent at pressures less than that required to produce crush-up (i.e., the quasi-elastic region). The Kayenta sandstone is the first rock of which we are aware that has a region in which σ_1 loading is apparently independent of strain rate. At pressures sufficient to initiate crush-up (Fig. 8), there is apparently a strain-rate effect. If we average the high-strain-rate experiments (3.5% strain), it appears that a 10^9 increase in loading rate increases shear strength (τ) by about 35%, or 4% per decade of rate. This is similar to the rate effects observed for failure in uniaxial stress loading.[6,13,18]

The initial loading moduli and the shear and compressional velocities derived therefrom are presented in Table 3. The agreement between initial loading moduli observed in uniaxial strain for single- and double-jacketed specimens indicates that the two jacketing procedures adopted here produce no discernible disparities. The agreement between loading moduli for uniaxial strain and uniaxial stress tests at confining pressures between 0.1 and 0.7 MPa is quite good also. The initial loading moduli in uniaxial strain for the sample seasoned to 300 MPa before strain gage installation are much stiffer, indicating

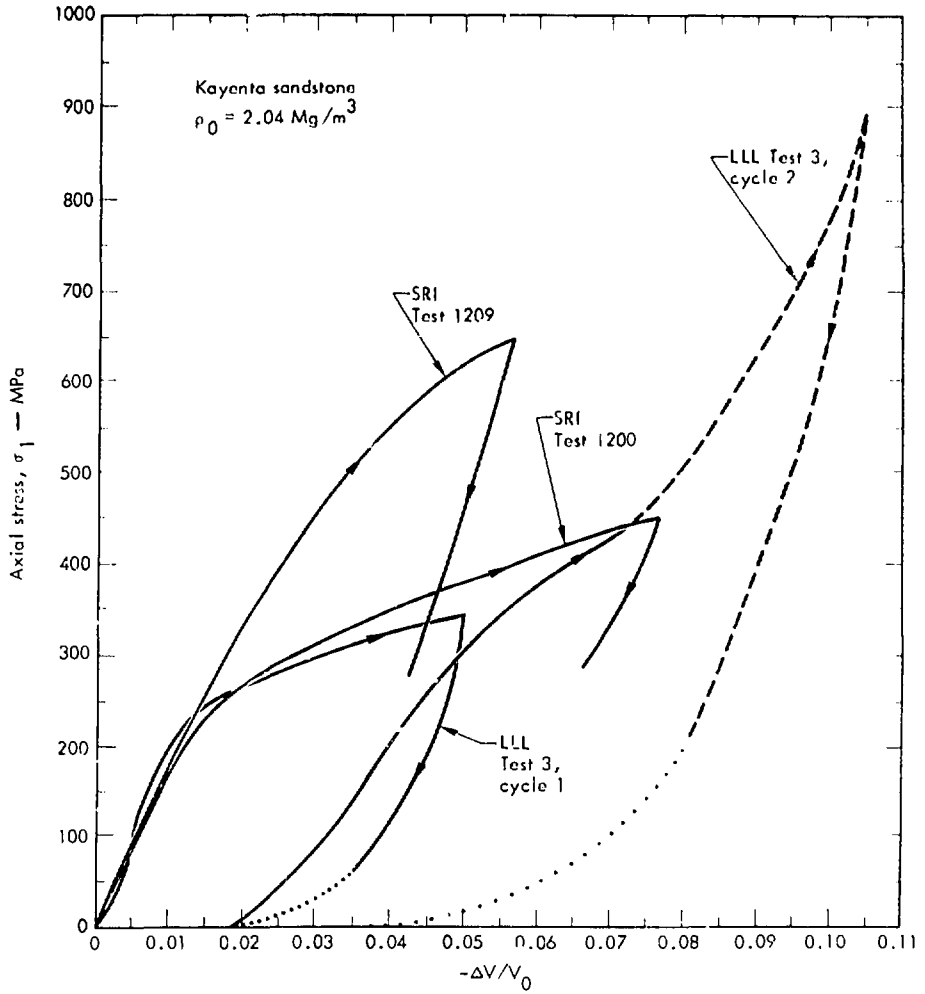

Fig. 9. Volume change as a function of axial stress (σ_1) in uniaxial strain loading (10^{-4}/s) for dry Kayenta sandstone. Also shown for comparison are SRI data for shock loading (10^5/s) (Ref. 17). Complete loading and unloading data for both cycles of test No. 3 (Table 3) are shown. Dotted portions of the uniaxial-strain unloading paths indicate hydrostatic unloading.

a possible loss of some initial porosity by either crush-up or crack closure.

The uniaxial stress tests indicate a possible maximum in initial shear and bulk moduli between 0.5 and 50 MPa. The decrease in moduli between 20 and 50 MPa may be related to the initiation of pore collapse in this weak, highly porous sandstone.

ULTRASONIC VELOCITY MEASUREMENTS

Ultrasonic velocities were calculated from travel times measured by a pulse-transmission technique[19] employing 1-MHz ceramic transducers. Samples were cylinders (19 mm in diameter by 25 mm long) encapsulated in a low-shear-strength polyurethane epon. For shear-wave travel-time measurements, 0.05-mm-thick copper disks were inserted between the transducers and rock to ensure reliable mechanical and electrical contact during crush-up. Data were corrected for the additional time delay through the copper disks. The measured shear and compressional travel times (t_s, t_p) are presented in Fig. 10; velocites (V_s, V_p) calculated using these travel times and the P-V relationship are plotted in Fig. 11.

Figure 11 indicates that V_p increases rapidly with an initial increase of confining pressure, presumably because of crack closure.[20] At about 10 MPa, however, V_p begins to decrease and has a local minimum at about 20 MPa. This small decrease in V_p (~4%) may be associated with local brittle failure at points of stress concentration within the sample. This occurs at a slightly lower mean pressure than where compaction toward the hydrostat is observed in uniaxial stress loading (Fig. 6). A discontinuity in V_p occurs at ~200 MPa, a pressure slightly lower than the beginning of the crush-up region of the P-V curve (Fig. 2). Although V_p does not show a decrease, the slope of the 100-to-200-MPa region is noticeably steeper than that at pressures greater than 300 MPa. The trend to increasing V_p during crush-up has been observed in a highly porous radiolarian earth,[21] sandstone and limestone,[22,23] and porous lunar material.[24]

The shear velocity also shows a large increase on initial application of confining pressure; however, no pronounced discontinuities in V_s are evident below 300 MPa. This is consistent with data on low-porosity rocks, which suggest that V_p is more sensitive than V_s to small changes in crack concentration.[25] In the region of gross crush-up of this sandstone, the shear velocity shows a slight decrease over a larger pressure interval than observed for V_p.

The velocity data indicate that the internal structure of the rock is undergoing change even at low confining pressure and that anomalous behavior occurs prior to the beginning of large-scale crush-up indicated by the P-V data. However, it should be emphasized that t_p, t_s, and the P-V relationship, which were used to calculate V_p and V_s, were not determined on the same sample but on different samples from the same block of sandstone.

The V_p and V_s calculated from travel-time measurements are higher than those calculated from initial uniaxial-stress and uniaxial-strain loading data at similar confining pressures, except at 20 MPa. At 20 MPa, a minimum occurs in the ultrasonic V_p and a maximum occurs in the V_p calculated from the quasi-static data. This discrepancy may be the result of cracks normal to σ_1, which are open at 20 MPa confining pressure but close as σ_1 is increased to the 20-to-40-MPa level, where the quasi-static velocities were calculated. This

possibility should be investigated by simultaneous measurement of V_p, V_s, and principal strains in this rock using the technique of Bonner et al.[25]

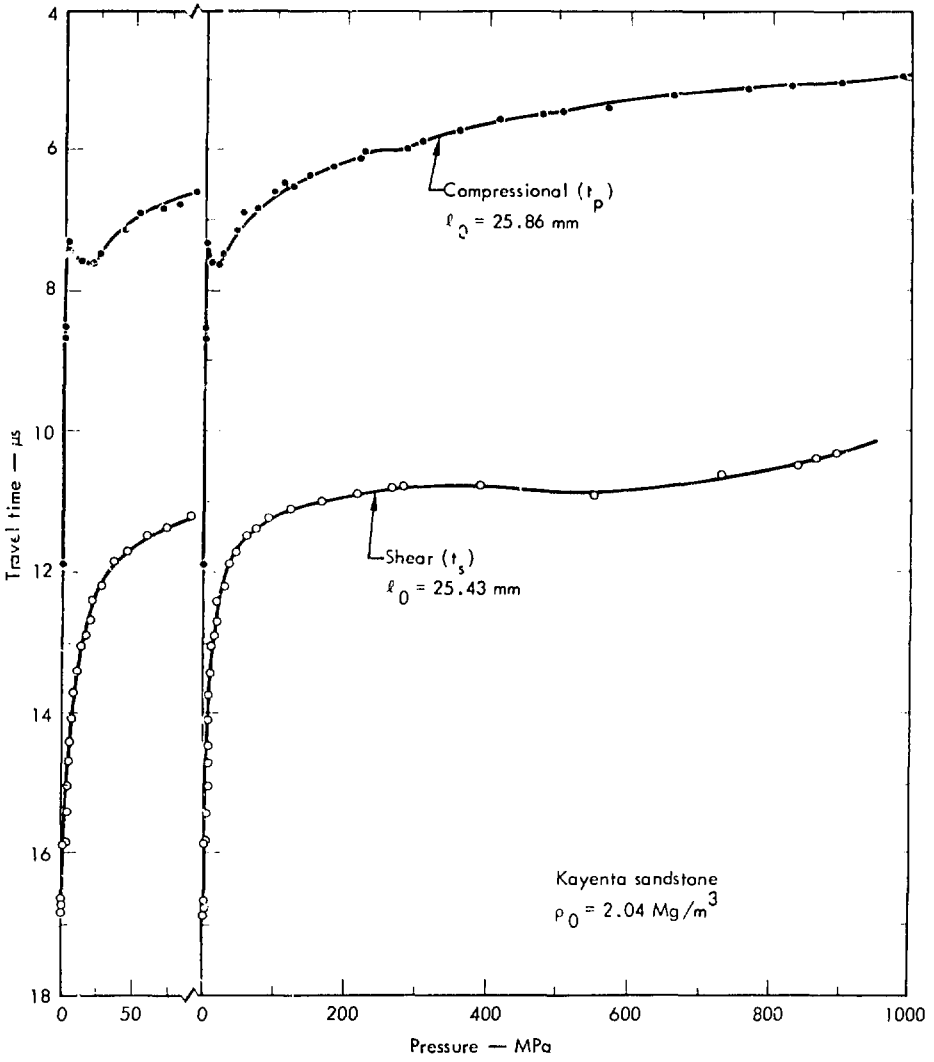

Fig. 10. Compressional- and shear-wave travel times as functions of confining pressure for dry Kayenta sandstone.

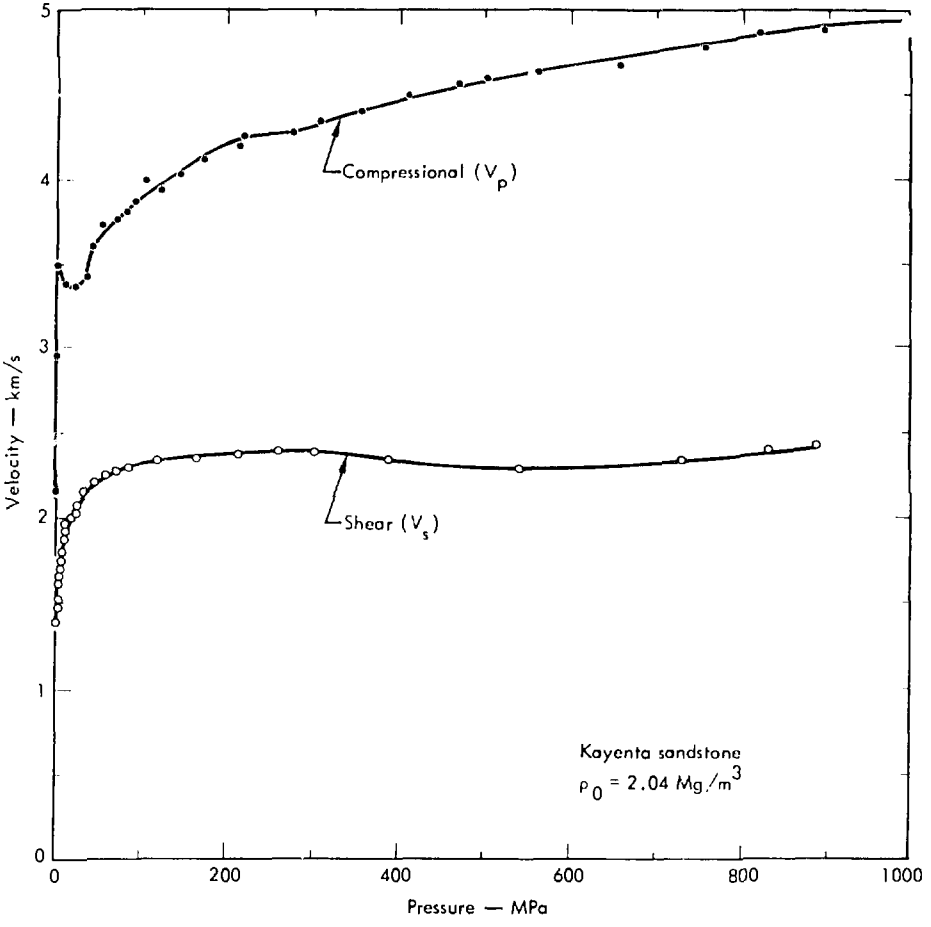

Fig. 11. Compressional and shear velocities as functions of confining pressure for dry Kayenta sandstone.

Acknowledgments

We thank R. Swift, Physics International, for supplying the samples and for valuable discussions. We thank N. Howard for helpful discussions of x-ray and grain-density studies. J. Ehrgott, Waterways Experiment Station, provided drafts of his reports on site geology and material properties prior to publication. Excellent technical assistance was provided by H. Washington, H. Stromberg, H. Louis, E. Lilley and E. Joslyn.

References

1. N. Howard, Lawrence Livermore Laboratory, private communication (1973).
2. R. N. Schock and A. G. Duba, Exp. Mech. 13, 43 (1973).
3. D. P. Stephens, E. M. Lilley, and H. Louis, Int. J. Rock Mech. Mining Sci. 7, 257 (1970).
4. J. Handin and R. V. Hager, Jr., Amer. Assoc. Petrol. Geol. Bull. 41, 1 (1957).
5. A. A. Giardini, J. F. Lakner, D. R. Stephens, and H. D. Stromberg, J. Geophys. Res. 73, 1305 (1968).
6. R. N. Schock, H. C. Heard, and D. R. Stephens, J. Geophys. Res. 78, 5922 (1973).
7. D. R. Stephens and E. M. Lilley, Proceedings of the Apollo 11 Lunar Science Conference, Vol. 3, 7427 (1970).
8. S. J. Green, S. W. Butters, A. H. Jones, and H. R. Pratt, The Stress-strain and Failure Response of Mixed Company Sandstone, Terra Tek, Inc., Salt Lake City, Utah, Rept. TR-72-33 (1972).
9. . Birch, Handbook of Physical Constants, Geol. Soc. Am. Mem. 47 (1966), p. 97.
10. H. C. Heard, R. N. Schock, and D. R. Stephens, High Pressure Mechanical] operties of Tuff From The Diamond Mine Site, Lawrence Livermore Laboratory, Re . UCRI -51099 (1971).
11. H. C. Heard, B. P. Bonner, A. G. Duba, R. N. Schock, and D. R. Stephens, High Pressure Mechanical Properties of Mt. Helen, Nevada, Tuff, Lawrence Livermore Laboratory, Rept. UCID-16261 (1973).
12. R. N. Schock, A. E. Abey, H. C. Heard, and H. Louis, Mechanical Properties of Granite From The Taourirt Tan Afella Massif, Algeria, Lawrence Livermore Laboratory, Rept. UCRL-51296 (1972).
13. J. Handin, H. C. Heard, and J. N. Magouirk, J. Geophys. Res. 72, 640 (1967).
14. R. N. Schock, H. C. Heard, and D. R. Stephens, Comparison of the Mechanical Properties of Graywacke Sandstones From Several Gas Stimulation Sites, Lawrence Livermore Laboratory, Rept. UCRL-51261 (1972).
15. A. G. Duba, A. E. Abey, and H. C. Heard, High Pressure Mechanical Properties of An Area 12, Nevada Test Site Tuff, Lawrence Livermore Laboratory, Rept. UCID-16377 (1973).
16. R. N. Schock and H. C. Heard, Static Mechanical Properties and Shock-Loading Response in Granite, Lawrence Livermore Laboratory, Rept. UCRL-74708 Preprint (1973)(to be published in J. Geophys. Res., 1974).
17. C. F. Petersen and D. C. Erlich, Dynamic Properties of Rock Required for Prediction Calculations, Stanford Research Institute, Menlo Park, Calif., Rept. DNA-3123F (1973).
18. W. F. Brace and A. H. Jones, J. Geophys. Res. 76, 4913 (1971).

19. R. N. Schock, H. Louis, and E. M. Lilley, The Determination of Acoustic Velocities and Dynamic Elastic Moduli in Rocks under Pressure, Lawrence Livermore Laboratory, Rept. UCRL-50750 (1969).

20. F. Birch, J. Geophys. Res. 66, 2199 (1961).

21. M. R. J. Wyllie, A. R. Gregory, and G. M. F. Gardner, Geophysics 23, 459 (1962).

22. R. N. Schock, H. C. Heard, and D. R. Stephens, Mechanical Properties of Rocks From Rio Blanco Gas Stimulation Experiments, Lawrence Livermore Laboratory, Rept. UCRL-51260 (1972).

23. P. N. LaMori, The Effects of Fluids and Cyclic Loading on the Elastic Moduli of Rocks, Battelle Columbus Labs, Columbus, Ohio, Annual Report, ARPA Order No. 1579 (1972).

24. H. Kanamori, A. Nur, D. Chung, and G. Simmons, Proceedings of the Apollo 11 Lunar Science Conference, Vol. 3, 2289 (1970).

25. B. P. Bonner, W. M. Benzing, and R. N. Schock, Trans. Am. Geophys. Union 54, 467 (1973).